UNIVERSITY OF BIRMINGHAM

A highly efficient synthetic process of graphene films with tunable optical properties

Han, Feng; Yang, Shuming; Jing, Weixuan; Jiang, Kyle; Jiang, Zhuangde; Liu, Huan; Li, Lei

Link to publication on Research at Birmingham portal

Accepted Manuscript

Author: Feng Han Shuming Yang Weixuan Jing Kyle Jiang
Zhuangde Jiang Huan Liu Lei Li

Please cite this article as: F. Han, S. Yang, W. Jing, K. Jiang, Z. Jiang, H. Liu, L. Li,
A highly-efficient synthetic process of graphene films with tunable optical properties,
Applied Surface Science (2014), http://dx.doi.org/10.1016/j.apsusc.2014.05.222

A highly-efficient synthetic process of graphene films with tunable optical properties

Feng Han[1], Shuming Yang[*][1], Weixuan Jing[1], Kyle Jiang[2], Zhuangde Jiang[1], Huan Liu[1], Lei Li[1]

[1]State Key Laboratory for Manufacturing Systems Engineering, Xi'an Jiaotong University, Xi'an, 710049, China

[2]School of Mechanical Engineering, University of Birmingham, Birmingham, B15 2TT, UK

Abstract: The paper reports an effective LB-based process to produce graphene oxide (GO). Uniform and controlled graphene oxide (GO) films were deposited on substrates by a simple and high-efficient Langmuir–Blodgett (LB)-based method. The influence of thermal reduction on GO films was systematically characterized and the annealing temperature of 800 □ was considered the most effective for reduction of GO. The optical and electrical properties were investigated for different reduced GO films to obtain the excellent sheet resistances of 440-620 Ω/sq with 60-70% range of light transparencies. A tunable surface wettability of GO films was found after heat treatment.

Keywords: graphene oxide films; Langmuir–Blodgett method; thermal reduction; optical properties

1. Introduction

Graphene, a one-atom-thick planar sheet of sp^2-bonded carbon atoms densely packed in a honeycomb crystal lattice, has become a rising star in material science recently [1,

[*] Corresponding author. Tel.: +862982668616; Fax: +86298266 8617.

E-mail address: shuming.yang@mail.xjtu.edu.cn.

2]. In contrast to monolayer graphene, graphene films, formed by few layers of graphene sheets, are widely used owing to the unusual physical properties such as high electron mobility, high thermal conductivity, and optimal mechanical properties. Significant attention has been paid to their applications in capacitors, flat displays, solar cells and sensors [3-6]. Recently, due to the high optical transmittance and electrical conductivity, a rapidly increasing interest has been focused on the graphene based films as an outstanding next-generation transparent conducting material in optoelectronic devices [7-11]. In addition, graphene films display the advantages of abundant sources, low-cost production, high mechanical strength, flexibility, and chemical stability. These properties make it possible for graphene films to replace the traditional electrodes such as indium tin oxide (ITO) and fluorine tin oxide (FTO) in the future.

The graphene sheets in current uses are relatively small, with the majority of their areas being a few hundreds of square micrometers [4, 9]. When a large area is covered by small graphene flakes, a large number of intersheet junctions are formed and numerous intersheet tunneling barriers are built, resulting in a high intersheet contact resistance. The fabrication of high-yield, large-size and uniform graphene films onto a substrate is the key to the success in putting the transparent conductive films into applications. Several methods have been reported on the fabrication of graphene films,

including mechanical cleavage of graphite, the epitaxial growth of graphene on SiC, the chemical vapor deposition (CVD) and reduction of GO. Mechanical cleavage of graphite tends to produce high quality graphene films with an area of hundreds of square millimeters, but it is limited by its low productivity [12]. Although producing graphene on SiC substrates is attractive for producing monolayer films [13], several hurdles prevent realist practical applications, such as low yield, small size, and the difficulty in transferring the films to other substrates. Moreover, the single crystal SiC substrate is of high cost. The CVD method is reported to be one of the most promising techniques for large-scale production of mono- or few-layer graphene films, although it requires specific substrates and has to be transferred to another substrate through chemical etching of the metal substrate [14, 15]. The ultrahigh vacuum conditions are also necessary to retain CVD growth.

Herein, we propose a highly-efficient process to produce uniform GO films on a solid substrate. The process starts by forming GO films using LB-based method, followed by thermal reduction of GO sheets with argon protection. Different thermal reduction temperatures result in different degrees of rGO and optical and electrical properties of the rGO films, making them potentially beneficial for transparent conductor in optoelectronic devices. In comparison to the aforementioned processes, reduction of GO is considered as an attractive approach for mass production of uniform graphene

films on any substrates, without further transfer of substrates [7-11]. In the formation of reduced GO (rGO), GO is considered as an important precursor of strong hydrophilicity for the preparation of transparent and conductive films using LB assembly.

Layer-by-layer assembly of multilayered films is now a well-established procedure for the construction of functional nanofilms [16]. The method, based on the alternate layer deposition of oppositely charged polyelectrolytes, indicates that electrostatic interaction is the main driving force for the construction of ultrathin films. As the LB assembly affords very thin films and high degree of structural order, it would constitute an excellent platform for the preparation of GO films in water surface without any surfactant or stabilizing agent [11, 17]. GO is an insulator and cannot be used as a conductive nanomaterial. The insulating GO has to be reduced to graphene through chemical treatment (e.g. hydrazine exposure) or thermal annealing in inert gases to render the material electrically conductive. It is discovered that hydrazine exposure for producing graphene sheets is insufficient to achieve largest reduction and easily introduces impurities, while thermal annealing results in an effective removal of oxygen from GO and introduces no impurities [4, 18, 19].

2. Experiment

GO powder was synthesized using the Hummers' method with some modifications

[20]. It was then admixed with methanol and deionized (DI) water (volume ratio of 5:1) at a concentration of 0.2 mg/ mL. The GO suspension was sonicated for 30 min to get a uniform dispersion and before being deposited onto a substrate by using LB technique [11, 17, 21]. Before the deposition the LB trough was thoroughly cleaned and the as-prepared 6mL GO solution was gently dropped onto the water subphase in the LB trough using a micro syringe. Compression was conducted by moving the two opposing sliding barriers towards each other at the speed of 10 mm/min. The surface pressure of the floating sheets was monitored by a tensiometer attached to a Wilhelmy platinum plate situated at the center of the trough. The GO sheets were transferred to a substrate at a specific stage of compression process by dip-coating method. The dried GO films on substrates were loaded inside a ceramic container, which was introduced into a furnace with controlled vacuum and gas flows. A vacuum of 0.1 Pa was established before heating. The sample were heated with a continuous flow of ultrapure argon at a rate of 10 □/min, held constant at different annealing temperatures (200, 300, 400, 500, 600, 700, 800, 900, 1000, and 1100 □) for an hour at 10^4 Pa, and were allowed to cool to room temperature with the furnace. At room temperature, ambient air was admitted to the furnace and the films were recovered. After the thermal treatment, GO sheets were reduced to rGO. In the experiments, 20× 10 mm silicon and glass substrates were cleaned for LB deposition of GO films. In

order to increase the hydrophilicity of the surface, the substrates were sonicated in a mixture solution (DI water: NH_4OH: H_2O_2=5:1:1) for 15 min, followed by rinsing repeatedly with DI water and drying in an oven for 30 min.

LB assembly of GO sheets was carried out on a commercial LB system (KSV-Minimicro 2000, KSV NIMA, Finland) and the reduction was conducted by Rapid thermal processor (BD26-RTP-500, Beijing Zhongxiyuanda Sci.-Tech. Co. Ltd., China). Atomic force microscope (AFM) (Innova, Veeco, USA) and scanning electron microscope (SEM) (SU-8010, Hitachi, Japan) were employed respectively to characterize the surface morphology of the samples. X-ray photoelectron spectroscopy (XPS) (AXIS ultra DLD, Shimadzu, Japan) and Raman spectroscopy (HR 800, Horiba Jobin Yvon, France) were used to characterize the graphitization of GO sheets. UV-Vis spectrophotometer (UV-3600, Shimadzu, Japan) and Four-point probes (RTS-8, Guangzhou Sitanzhen Sci.-Tech. Co. Ltd., China) were utilized for analysis of optical properties.

3. Results and discussions

3.1 LB assembly of controlled GO structure

The controlled GO structures prepared by LB assembly are illustrated in Fig. 1. The typical isothermal surface pressure/area curve shown in Fig. 1e depicts that the surface pressure gradually increased as the two opposing barriers moved towards each

other for more compression. During the compression process there was a change in the slope corresponding to the phase transition of GO sheets from gas to condensed liquid and to solid state. In order to find the effect of surface pressure on GO assembly, GO sheets were transferred to substrates at different stages of compression. The SEM images of four different styles of GO structures were presented in Figs. 1a-d. At the very beginning of LB assembly without compression, the separate GO sheets tiled uniformly over the water subphase and the surface pressure maintained zero (Fig. 1a). The opposing barriers started to move towards each other and the separate GO sheets became closely-packed (Fig. 1b), resulting in an increased surface pressure. While the barriers moved continuously for further compression (Fig. 1c), the floating GO sheets were over-packed and overlapped. It is noteworthy that the GO monolayer stacked into multilayered sheets for face-to-face interaction at a higher pressure (Fig. 1d). The water color gradually became dark as the compression continued. To clarify highly reversibility and stability against compression, surface pressure vs. area curves for two sequential compression-expansion cycles are illustrated in Fig. 1f. It is evident that the curves are of the similar shape except a small amount of carbon loss from the second compression [17].

3.2 Surface morphology of GO films

Since the SEM images are representative of electronic structure, not topography, AFM is needed to establish the thickness and surface roughness of films. Fig. 2a is a representative AFM image of the GO sheets obtained before compression in the LB assembly. The thicknesses of the GO sheets with wrinkled edges are 4.2, 2.3, 1.3 and 1.3 nm from 1 to 4, as plotted in Fig. 2b, measured by scanning the line as shown in Fig. 2a, respectively. Since the thickness of GO monolayer is approximately 1 nm as reported previously [22, 23], it is indicated that the as-prepared GO sheets have been flaked into some layers of GO sheets..The arithmetical mean roughness of as prepared GO and rGO films after thermal treatment are summarized in Fig. 2c. The inset shows the increasing thickness of films obtained at increasing surface pressure. The surface roughness increases with the increase of the thickness of GO films, which are attributed to the layer-by-layer deposition of uneven GO sheets and accumulated wrinkles. It is worth noting that the surface roughness of GO films are consistently reduced after the thermal treatment due to the removal of oxygenated functional groups and graphitization of the films [11].

3.3 Thermal reduction of GO films

GO is transformed from modified-graphene with oxygen functional groups in the form of epoxy and hydroxy groups on the basal plane and carboxyl and acetate groups at the edges [24,25]. The reduction is conducted through pyrolysis of oxygenated

groups and retrieval of C-C bonding. Fig. 3a-d show the typical C1s XPS spectra of

as-prepared GO and GO annealed at 200, 800 and 900 □ in argon, respectively. Curve

fitting of the C1s spectra was performed using commercial software Avantage,

indicative of the C1s signals of the original GO deconvoluted into several signals for

C-C bond (~284.5 eV), C-O bond (~286.2 eV), C=O bond (~287.8 eV), O-C=O bond

(~288.9 eV), and O-CO-O bond (~290.8 eV). The effect of increased reduction

temperature on (C-C) % content and the values of C/O ratio are illustrated in Fig. 3

(e), respectively. Compared with (C-C) % content corresponding to sp^2 carbon

fraction in as-synthesized GO (57.93%), it was greatly improved to 73.44% with the

annealing temperature at 200 □. However, no significant change in (C-C) % content

was observed until the temperature continued to increase to 800 □. The maximum (C-

C) % content (94.59%) was obtained at the reduction temperature of up to 1000 □. In

addition, with the increased reduction temperature, the trends of C/O ratio values were

observed to firstly increase and then decrease. The C/O ratio changes in Fig. 3e can be

explained from the mass loss of GO upon heating that, GO is thermally unstable and

starts to lose mass upon heating even below 100 □ because of desorption of bound

water. The majority mass loss occurs between 190~240 □ resulting from thermal

decomposition of oxygen functional groups [26]. Annealing at elevated temperatures

further removes the residual oxygen from GO and breaks down the defect carbon (e.g.

ethyl). Ultimately the carbon skeleton of GO is greatly decomposed above 800 ☐ [22].

The best reduction process can be obtained by the largest decomposition of oxygen

functional groups and the simultaneous restoration of sp^2 C–C bonds as complete as

possible. It was decided by higher (C-C) % content (84.43%) and meanwhile larger

C/O ratio value (20) that efficient reduction of GO thin films can be therefore

achieved upon 800 ☐. The remaining oxygen-containing groups in reduced GO, the

majority of which consisted of C-O bonds, were difficult to be removed by thermal

annealing [27]. In contrast to reduction at a relative high temperature (550 ☐)

mentioned in previous reports [4], this method provides a controllable, gradual

transformation from GO to rGO with an initially reduced temperature at 200 ☐.

The significant structural changes of the obtained rGO were further investigated by

Raman spectroscopy with 514 nm laser excitation. Considering of the predominant

mass loss of carbon skeleton upon heating over 800 ☐, thermal annealing conducted

more than 800 ☐ did not benefit the reduction of GO and it was not shown in our

Raman spectra. Fig. 4a & b exhibit the typical Raman spectra of GO and rGO

annealed at 200, 400, 600, 800 ☐, respectively. Two major .lpeaks at ~1365 and

~1590 cm^{-1}, corresponding to D and G, were displayed in Fig. 4a. The prominent D

peak may be attributed to the structural imperfections resulting from disordered

carbon [28], while G peak, corresponding to the first-order scattering of the E_{2g} mode,

originates from sp^2-hybridized carbon. Fig. 4c shows the influence of reduction temperature on G peak position and FWHM, respectively. Compared with that of GO thin films, the rGO peak positions were discovered to be red-shifted to lower frequency, while the full width at half-maximum (FWHM) of G peak were broadened. The maximum redshift and widening value was ~9 $cm^{-1}$and ~32 cm^{-1}, respectively. The observation can be explained that there are sp^2 carbon clusters of a few nanometers in GO isolated within a defective carbon lattice or highly disordered sp^3 matrix. During reduction by heat treatment, numerous oxygen-containing functional groups are removed and new graphitic domains of sp^2 clustering in some defective carbon lattices are formed. The GO with amorphous and highly disordered sp^3 matrix is transformed to nanocrystalline graphene. Thus the transformation leads to the redshift and broadening of the G peak. Fig. 4b shows two other peaks called 2D and (D+G) at 2600-3000 cm^{-1}, which are often ignored owing to the weak intensities compared to D and G peak. The 2D peak represents the crystallization of graphitic materials and ascribes to an out-of-plane vibration mode, and (D+G) peak is induced as a result of lattice disorders. Notably, the peak intensity ratios of D/G and 2D/(D+G), as reflections of the recovery of sp^2 fraction size in GO obtained at different stages of reduction, both increased after deoxygenation by reduction as shown in Fig. 4d. The increased D/G intensity ratios in rGO at different reduced

stages suggest structural disorders compared to that in GO, owing to a decrease in the average size of initially present sp^2 domains and the creation of newly formed small but numerous sp^2 clusters upon reduction [29]. However, the small changes of D/G intensity ratios are less sensitive to distinguish the recovery of electronic conjugation of GO than that of 2D/(D+G) ratios [11]. Thus it is more convenient for us to observe the changes via comparing the two peaks of 2D and (D+G). Moreover, It is worth noting that the 2D/(D+G) ratio at low reduction temperature of 200 □ is deeply increased while no significant changes are observed until an higher temperature is applied, which basically agrees with the above XPS results. From the XPS and Raman spectra the effect of heat treatment on the GO reduction is observed that reduction can be moderately operated upon heating at the low temperature of 200 □, and high temperature at 800 □ are required to further remove the oxygen-containing functional groups and restoration of sp^2 fraction in GO.

3.4 Optical properties and surface wettability of rGO

The optical transmittance properties at λ= 550 nm of GO prepared with different thickness at different reduction temperature are summarized in Fig. 5 (a). It can be seen that there was a distinct transmittance difference between GO and annealed GO. Higher surface pressure resulted in thicker films which show lower transparency after heat treatment due to a higher degree of light absorption. The annealed (800 □) GO

thin films change color from light brown to dark black, indicating partial restoration of π-electron network in GO, and thus a decrease in the transparency [9]. The transparency of all the samples was observed to improve above 800 □ owing to the substantial amount of carbon loss at a relatively high temperature. Fig. 5b shows the corresponding transmittances as a function of the GO thin films with controlled temperature treatment obtained at surface pressure of 15 mN/m, and the sheet resistance is plotted in the inset. The flat transmittance spectra across visible and near-infrared region make graphene outstanding for the optoelectronic applications. Annealing at different temperatures in argon led to a dramatic decrease in the sheet resistances in the range of 440-620 Ω/sq with the film thickness of 37.8 nm, which were much lower than that of GO thin films measured at 45 KΩ/sq with the same thickness. This measured values of sheet resistance were expected and similar to those reported in the literature [11,30]. The sheet resistance increased by approximately two orders of magnitude for a thickness of 37.8 nm after thermal annealing. The heat treatment removed partial oxygen-containing functional groups and promoted graphitization of GO films, suggesting that the transparency and sheet resistances of GO films was relevant to the restoration of π-electron system in GO.

Generally, contact angle is often employed to analyze the surface wettability of thin films. Fig. 6 clearly indicated that the contact angle was changed in the range of 20-

73^0, suggesting a tunable surface wettability of GO films upon heating. Due to many factors such as surface contamination, roughness and surface heterogeneity can affect the contact angle, it was insufficient to show relationships between the contact angle and the different heat treatment and further study would be needed in the future. Undoubtedly, it provides the possibility to make GO thin films excellent as optoelectronic materials (e.g. solar cells) for their tunable surface wettability.

4. Conclusions

An effective LB-based method to produce GO films was reported and the relative effects of thermal reductive temperatures on the optical performance of the films were investigated. GO films were deposited on a solid substrate with the sheets density continuously tunable from separate, close-packed to over-packed. The fabrication followed by thermal reduction provided a good way to make large-size transparent conductive films.The graphitization conditions by changing the thermal temperatures were identified and highly transformation from GO to rGO was conducted at the temperature as low as 200 □. The optical transmittance of films made from separate, close-packed to over-packed GO sheets were decreased with the increasing thickness. Compared to the film made from GO sheets with the same thickness, the transmittance of rGO films were much lower after thermal reduction treatment. The potential of highly rGO thin films as transparent conductors was evaluated by

measuring the optical transmittances and electrical conductivities of rGO thin films with the thickness of 37.8 nm. The transparent conductors made from rGO films in this study showed the excellent sheet resistances of 440-620 Ω/sq at the transmittance of 60-70% range with the tunable surface wettability.

Acknowledgements

Reference

[1] K. S. Novoselov, A. K. Geim, S. V. Morozov, D. Jiang, Y. Zhang, S. V. Dubonos, I. V. Grigorieva, A. A. Firsov, Electric field effect in atomically thin carbon films, Science 306 (2004) 666-669.

[2] A. K. Geim, K. S. Novoselov, The rise of graphene, Nat. Mater. 6 (2007) 183-191.

[3] X. Wang, L. J. Zhi, N. Tsao, Z. Tomovic, J. L. Li, K. Mullen, Transparent carbon films as electrodes in organic solar cells, Angew. Chem. 120 (2008) 3032-3034.

[4] X. Wang, L. J. Zhi, K. Mullen, Transparent, conductive graphene electrodes for dye-sensitized solar cells, Nano Lett. 8 (2008) 323-327.

[5] Y. P. Zhang, H. B. Li, L. K. Pan, T. Lu, Z. Sun, Capacitive behavior of graphene– ZnO composite film for supercapacitors, J. Electroanal. Chem. 634 (2009) 68-71.

[6] F. Schedin, A. K. Geim, S. V. Morozov, E. W. H ill, P. Blake, M. I. Katsnelson, K. S. Novoselov, Detection of individual gas molecules adsorbed on graphene, Nat Mater. 6 (2007) 652-655.

[7] T. Szabo, A. Szeri, I. Dekany, Composite graphitic nanolayers prepared by self-assembly between finely dispersed graphite oxide and a cationic polymer, Carbon 43 (2005) 87-94.

[8] T. Szabo, A. Bakandritsos, V. Tzitzios, E. Devlin, D.Petridis, I. Dekany, Magnetically Modified Single and Turbostratic Stacked Graphenes from Tris (2, 2 -bipyridyl) Iron (II) Ion-Exchanged Graphite Oxide, J. Phys. Chem. B 112 (2008) 14461-14469.

[9] H. A. Becerril, J. Mao, Z. F. Liu, R. M. Stoltenberg, Z. N. Bao, Y. S. Chen, Evaluation of solution-processed reduced graphene oxide films as transparent conductors, Y. Chen, ACS Nano 2 (2008) 463-470.

[10 S. J. Wang, Y. Geng, Q. B. Zheng, J. K. Kim, Fabrication of highly conducting and transparent graphene films, Carbon 48 (2010) 1815-1823.

[11] Q. B. Zheng, W. H. Ip, X. Y. Lin, N. Yousefi, K. K. Yeung, Z. G. Li, J. K. Kim, Transparent conductive films consisting of ultralarge graphene sheets produced by Langmuir_Blodgett assembly, ACS Nano 5 (2011) 6039-6051.

[12] J. C. Meyer, A. K. Geim, M. I. Katsnelson, K. S. Novoselov, T. J. Booth, S. Roth, The structure of suspended graphene sheets, Nature 446 (2007) 60-63.

[13] K. V. Emtsev, A. Bostwick, K. Horn, J. Jobst, G. L. Kellogg, L. Ley, J. L. McChesney, T. Ohta, S. A. Reshanov, J. Rohrl, Towards wafer-size graphene layers by atmospheric pressure graphitization of silicon carbide, Nat. Mater. 8 (2009) 203-207.

[14] A. Reina, X. Jia, J. Ho, D. Nezich, H. Son, V. Bulovic, M. S. Dresselhaus, J. Kong, Large area, few-layer graphene films on arbitrary substrates by chemical vapor deposition, Nano Lett. 9 (2009) 30-35.

[15] K. S. Kim, Y. Zhao, H. Jang, S. Y. Lee, J. M. Kim, K. S. Kim, J. H. Ahn, P. Kim, J. Y. Choi, B. H. Hong, Large-scale pattern growth of graphene films for stretchable transparent electrodes, Nature 457 (2009) 706-710.

[16] T. Szabo, M, Szekeres, I. Dekany, C. Jackers, S. D. Feyter, C. T. Johnston, R. A. Schoonheydt, Layer-by-layer construction of ultrathin hybrid films with proteins and clay minerals, J. Phys. Chem. C 111 (2007) 12730-12740.

[17] L. J.Cote, F. Kim, J. X. Huang, Langmuir-Blodgett assembly of graphite oxide single layers, J. Am. Chem. Soc. 131 (2009) 1043-1049.

[18] C. Gomez-Navarro, R. T. Weitz, A. M. Bittner, M. Scolari, A. Mews, M. Burghard, K. Kern, Electronic transport properties of individual chemically reduced graphene oxide sheets, Nano Lett. 7 (2007) 3499-3503.

[19] S. Stankovich, R. D. Piner, X. Q. Chen, N. Q. Wu, S. T. Nguyen, R. S. Ruoff, Stable aqueous dispersions of graphitic nanoplatelets via the reduction of exfoliated graphite oxide in the presence of poly(sodium 4-styrenesulfonate), J. Mater. Chem. 16 (2006) 155-158.

[20] W. S. Hummers, Jr., R. E. Offeman, Preparation of graphitic oxide, J. Am. Chem. Soc. 80 (1958) 1339.

[21] Y. Gao, X. Q. Chen, H. Xu, Y. L. Zou, R. P. Gu, M. S. Xu, A. K. Y. Jen, H. Z. Chen, Highly-efficient fabrication of nanoscrolls from functionalized graphene oxide by Langmuir–Blodgett

method, Carbon 48 (2010) 4475-4482.

[22] S. Stankovich, D. A. Dikin, R. D. Piner, K. A. Kohlhaas, A. Kleinhammes, Y. Y. Jia, Y. Wu, S. T. Nguyen, R. S. Ruoff, Synthesis of graphene-based nanosheets via chemical reduction of exfoliated graphite oxide, Carbon 45 (2007) 1558-1565.

[23] M. J. McAllister, J. L. Li, D. H. Adamson, H. C. Schniepp, A. A. Abdala, J. Liu, M. Herrera-Alonso, D. L. Milius, R. Car, R. K. Prud'homme, I. A. Aksay, Single sheet functionalized graphene by oxidation and thermal expansion of graphite, Chem. Mater. 19 (2007) 4396-4404.

[24] T. Szabo, O. Berkesi, P. Forgo, K. Josepovits, Y. Sanakis, D. Petridis, I. Dekany, Evolution of surface functional groups in a series of progressively oxidized graphite oxides, Chem. Mater. 18 (2006) 2740-2749.

[25] Virendra Singh, Daeha Joung, Lei Zhai, Soumen Das, Saiful I. Khondaker, Sudipta Seal, Graphene based materials: Past, present and future, Prog. Mater. Sci. 56 (2011) 1178-1271.

[26] G. C. Wang, Z. Y. Yang, X. W. Li, C. Z. Li, Synthesis of poly(aniline-co-o-anisidine)-intercalated graphite oxide composite by delamination/reassembling method, Carbon 43 (2005) 2564-2570.

[27] D. X. Yang, A. Velamakanni, G. Bozoklu, S. Park, M. Stoller, R. D. Piner, S. Stankovich, I. Jung, D. A. Field, C. A. V. Jr, R. S. Ruoff, Chemical analysis of graphene oxide films after heat and chemical treatments by X-ray photoelectron and Micro-Raman spectroscopy, Carbon 47 (2009) 145-152.

[28] W. T. Zheng, Y. M. Ho, H. W. Tian, M. Wen, J. L. Qi, Y. A. Li, Field emission from a composite of graphene sheets and ZnO nanowires, J. Phys. Chem. C 113 (2009) 9164-9168.

[29] G. Eda, Y. Y. Lin, C. Mattevi, H. Yamaguchi, H. Chen, I. S. Chen, C. W. Chen, M. Chhowalla, Blue photoluminescence from chemically derived graphene oxide, Adv. Mater. 22 (2010)505-509.

[30] Q. B. Zheng, M. M. Gudarzi, S. J. Wang, Y. Geng, Z. G. Li, J. K. Kim, Improved electrical and optical characteristics of transparent graphene thin films produced by acid and doping treatments, Carbon 49 (2011) 2905-2916.

Captions of the figures:

FIG. 1 (a-d) SEM images of GO films obtained at four different surface pressures corresponding to four different stages of GO formation, respectively. (e) The typical isothermal surface pressure vs area curve. (f) Isotherm plots of two sequential compression-expansion cycles.

FIG. 2 (a) A representative AFM image of GO sheets on a silicon wafer obtained without compression in LB assembly. (b) A depth profile in a line scans of the GO sheet as indicated in (a). (c) The arithmetical mean roughness of GO prepared at different surface pressure with different reduction temperature. The thickness of GO films as a function of surface pressure is plotted in the inset.

FIG. 3 Typical C1s XPS spectra for materials at some different reduction temperatures: (a) unreduced GO, (b) 200 , (c) 800 , (d) 900 . (e) (C-C) % content and the values of C/O ratio as a function of the annealing temperature, respectively.
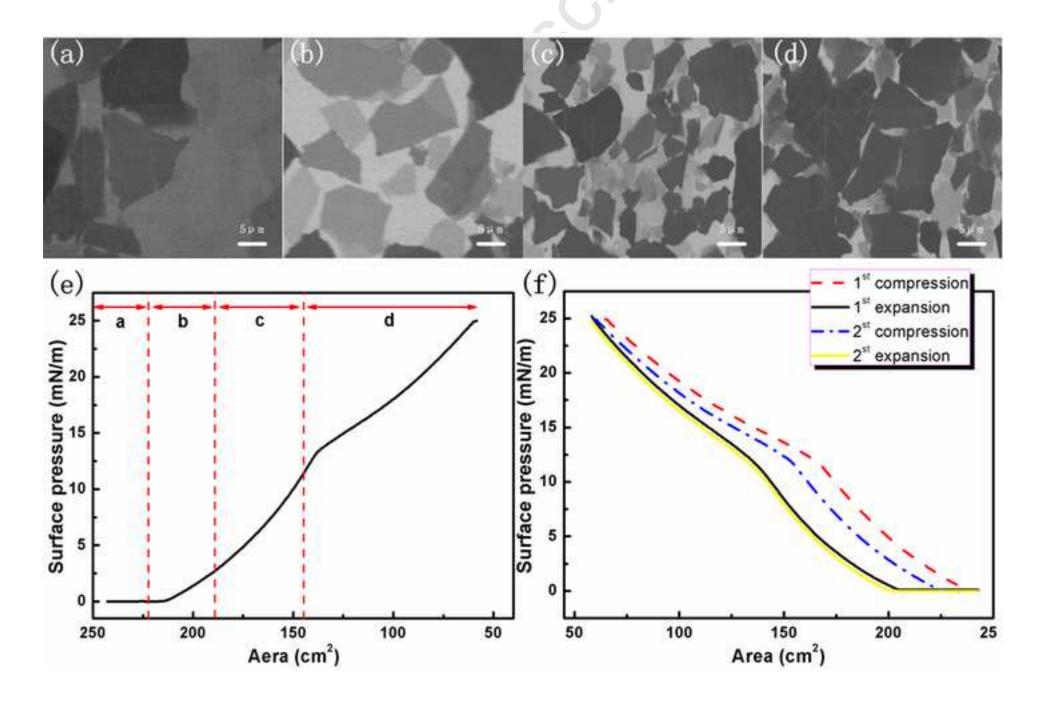
FIG. 4 (a) & (b) are Raman spectra for GO, rGO-200, rGO-400, rGO-600 and rGO-800. (c) G peak and FWHM as a function of annealing temperature. (d) The intensity ratio of D/G and 2D/(D+G) as a function of annealing temperature.
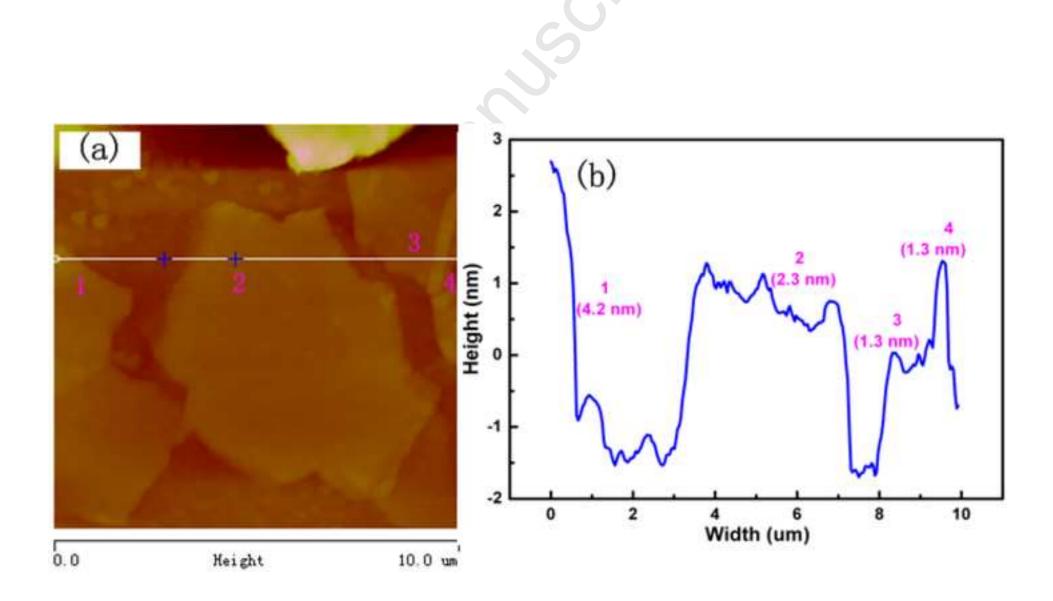
FIG. 5 (a) the optical transmittance properties at λ= 550 nm of GO prepared with different thickness of films under different reduction treatment. (b) The corresponding transmittances of GO thin films obtained at surface pressure of 15 mN/m upon different heating treatment. The sheet resistance (with error bars) for as prepared GO films and rGO thin films under different thermal reduction is plotted in the inset.
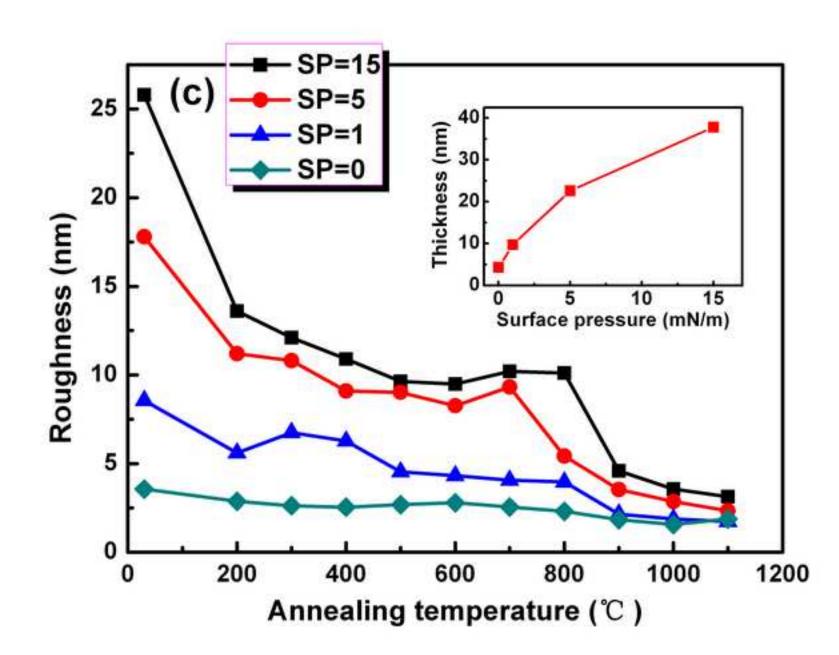
FIG. 6 The effect of the contact angle of GO films obtained at surface pressure of 15 mN/m on the different annealing temperatures. The inset is a photograph of measured contact angle.
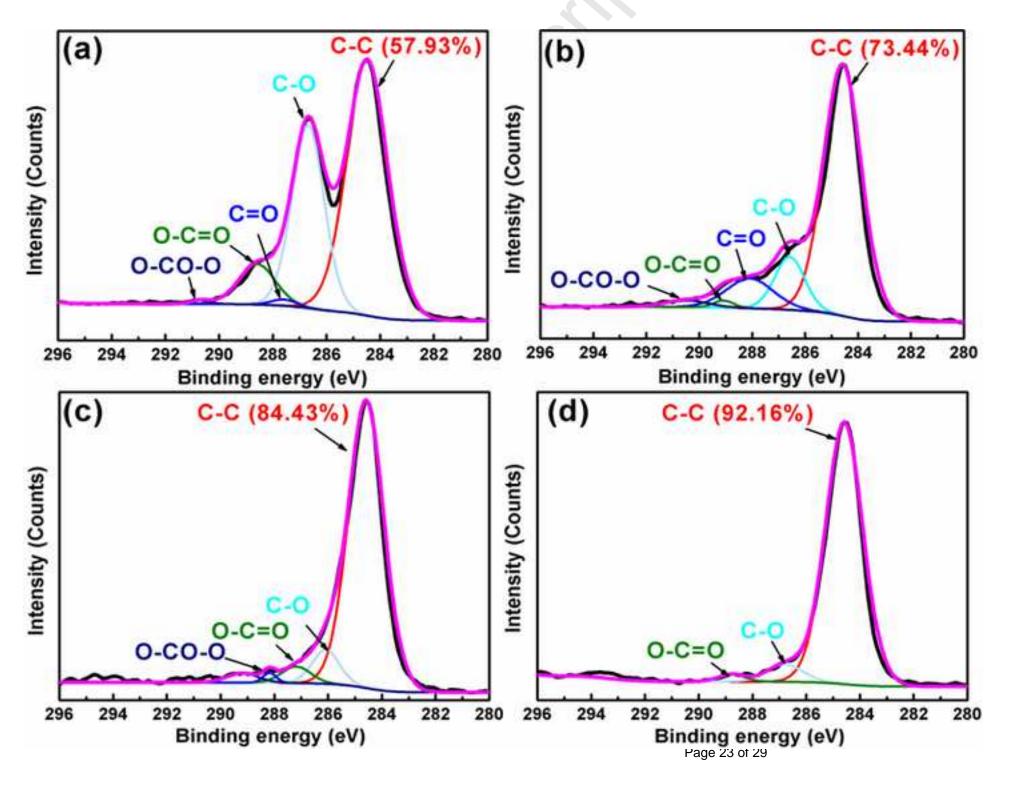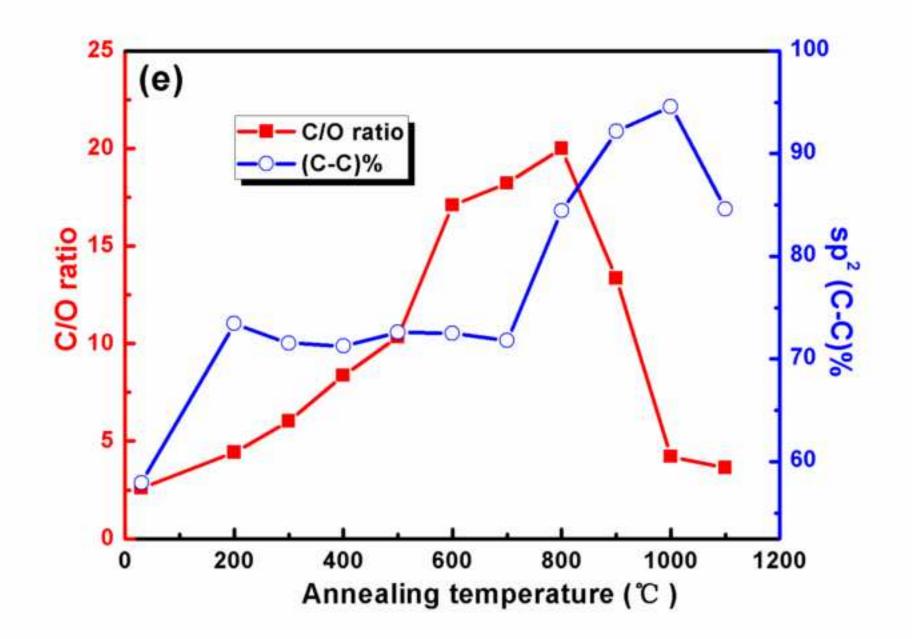
Highlights

- Uniform and controlled graphene oxide films were deposited on substrates using Langmuir–Blodgett (LB)-based method.
- The influence of thermal reduction on GO films was systematically characterized.
- 800   was considered the most effective for reduction.
- The optical properties were investigated for different reduced GO films.
- A tunable surface wettability of GO films was found after heat treatment.

Figure

Figure